J Wood Sci (2011) 57:484–492
DOI 10.1007/s10086-011-1198-6

ORIGINAL ARTICLE

Takahisa Kamada · Motoi Yasumura · Shimpei Yasui
Luc Davenne · Motoi Uesugi

Pseudodynamic tests and earthquake response analysis of timber structures III: three-dimensional conventional wooden structures with plywood-sheathed shear walls

Received: February 20, 2011 / Accepted: April 15, 2011 / Published online: August 2, 2011

Abstract Pseudodynamic (PSD) tests were conducted on plywood-sheathed conventional Japanese three-dimensional (3D) wooden structures. Lateral load was applied to the edge beam of specimen structures to generate eccentricity loading. Specimens were based on a combination of shear walls with openings in the loading direction and horizontal diaphragms with different shear stiffness. The principle deformation of the horizontal diaphragm was torsion for rigid diaphragms and shear deformation for flexible diaphragms. Lumped-mass time-history earthquake response analysis was conducted on the tested structures, and additional calculations were conducted on structures with different eccentricity rates. Dynamic analyses were conducted by varying the masses and the resistance of the walls in the loading direction. The simulated peak displacement response in the loading plane agreed comparatively well with the PSD test results. The maximum displacement response on changing the wall resistant ratio showed almost the same tendency as that obtained by changing the mass ratio up to an eccentricity rate of 0.3; however, the maximum displacement response increased markedly beyond an eccentricity rate of 0.4. It was proved that the lumped-mass 3D model proposed in this study was appropriate for conducting a parameter study on the 3D dynamic behavior of timber structures.

Key words Computer online control · Lumped-mass model · Dynamic analysis · 3D Structures · Plywood sheathing

T. Kamada (✉)
United Graduate School of Agricultural Science, Gifu University, 836 Ohya, Suruga-ku, Shizuoka 422-8529, Japan
Tel. +81-54-237-1111; Fax +81-54-237-3028
e-mail: t-kamada-shizuoka@live.jp

M. Yasumura
Faculty of Agriculture, Shizuoka University, Shizuoka 422-8529, Japan

S. Yasui
Research and Development Center, DAIKEN Corporation, Okayama 702-8045, Japan

L. Davenne
Laboratoire de Mecanique et Technologie, ENS Cachan, 94235 Cachan, France

M. Uesugi
Miyazaki Prefecture Wood Utilization Research Center, Miyakonojo, Miyazaki 885-0037, Japan

Part of this article was presented at the Annual Meeting of the Japan Wood Research Society, Fukuoka, March 2004, and Meeting Thirty-seven of CIB-W18, Edinburgh, September 2004

Introduction

The influence of eccentricity wall layout and mass distribution on the seismic performance of timber structures is of relevance to the design of timber structures. A number of experimental and theoretical studies have been conducted on this subject, but few have dealt with the influence of the in-plane shear stiffness on the seismic behavior of timber structures. Therefore, it is of great importance to develop a comparatively simple method to predict the behavior of three-dimensional (3D) structures and to validate this method by a simplified testing method. We consider that pseudodynamic (PSD) testing is an appropriate method for this purpose as this test method requires relatively simple apparatus and measuring system comparing to shake-table tests.[1–3] In this study, small 3D structures were subjected to eccentricity pseudodynamic loads simulating the seismic response, and the experimental results were compared with the results of time history earthquake response analysis including a shear stiffness matrix for the horizontal diaphragm and the lumped-mass model for the shear walls. The hysteresis model of shear walls proposed in previous studies[4–6] was applied to the simulation, and the pseudodynamic test results showed that the 3D model proposed in this study predicted well the three-dimensional behavior of timber structures with either a rigid or flexible horizontal diaphragm.

Specimens

Japanese conventional post and beam structures with plywood-sheathed shear walls and a horizontal diaphragm

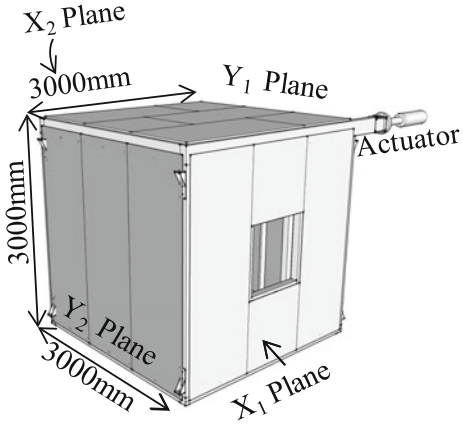

Fig. 1. Configuration of the specimen structure

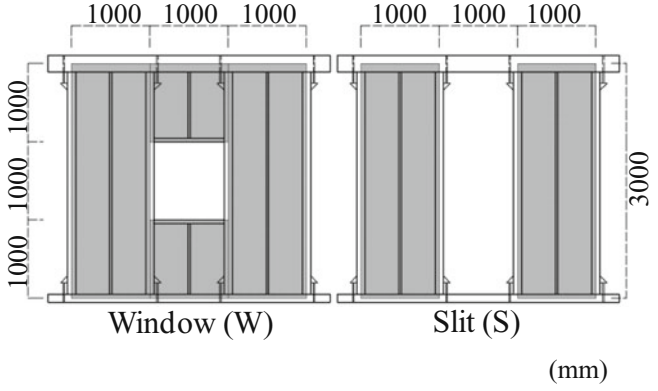

Fig. 2. Configuration of window (*W*) wall and slit (*S*) wall

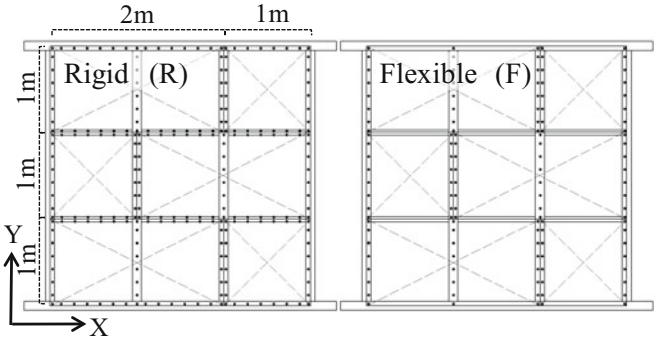

Fig. 3. Frame and nail patterns for rigid (*R*) and flexible (*F*) diaphragms. In rigid diaphragms, sheets are nailed on beams, joists, and bridging joists; in flexible diaphragms, sheets are not nailed on beams or bridging joists

Table 1. Specimen structures that underwent pseudodynamic testing

Specimen	X_1 plane	X_2 plane	Horizontal diaphragm
WW-R	W (Window)	W (Window)	R (Rigid)
WW-F			F (Flexible)
WS-R	W (Window)	S (Slit)	R (Rigid)
WS-F			F (Flexible)

were prepared for the PSD tests. Figure 1 gives a general depiction of the specimen and test setup. Specimens had the shape of a cube 3 m on an edge. Posts, sills, and joists were 105 × 105-mm spruce (*Picea* spp.) glued laminated timber complying with JAS E85-F300, and beams were 105 × 210-mm spruce glued laminated timber complying with JAS E95-F270. Studs and headers were 30 × 105-mm and 45 × 10-mm spruce lumber, respectively. Posts placed every 1000 mm were connected to the sill and beam with a steel pipe of 26.5 mm diameter and hold-down connections.[7] Studs placed at the center between posts were fastened to the sill and beam with two N75 nails at both ends of the studs. Joists were connected to the beam by metal joist hangers spaced 1000 mm apart. Each sill was anchored to the steel base frame with three M16 bolts positioned at the center and 150 mm inside from the ends. Seven-and-a-half-millimeter-thick, 1000-mm-wide, and 3000-mm-long lauan plywood of JAS Grade 1[8] with a density of 880 kg/m^3 was sheathed on the wall frames with N50 nails at intervals of 150 mm.

Walls parallel to the loading direction in the X_1 and X_2 planes had an opening of window configuration (1 m wide and 1 m height) (W) or an opening 1 m wide and 3 m high at the center of the wall (S), as shown in Fig. 2; walls perpendicular to the loading direction in the Y_1 and Y_2 planes had no openings. Specimen WW had walls W on both X_1 and X_2 planes, and specimen WS had a wall W in the X_1 plane and a wall S on the X_2 plane. Figure 3 shows the details of the horizontal diaphragm. A horizontal diaphragm of 3 × 3 m^2 consisted of 105 × 210-mm beams and 105 × 105-mm joists spaced 1000 mm apart. Twenty-four-millimeter-thick *sugi* plywood of JAS Grade 2, 1000 mm wide and 2000 mm long, was sheathed on the floor frame with N75 nails at intervals of 150 mm. Two kinds of diaphragm with different in-plane shear stiffness were prepared. A rigid horizontal diaphragm (R) in which all the edges of the plywood sheathing were nailed to the beams, joists, and 60 × 60-mm bridging joists placed at the plywood joints was prepared to provide comparatively high shear stiffness, and a flexible diaphragm (F) in which all nails on the longitudinal edges of the plywood were omitted was expected to have a lower shear stiffness. Table 1 summarizes the specimens based on the combination of wall types in the X_1 and X_2 planes and horizontal diaphragms of different shear stiffness.

Test methods

Racking test of the horizontal diaphragm

Racking tests of the horizontal diagram were conducted to determine the parameters for modeling the load–displacement relationships. The same types of floor (R and F) were prepared, except that the beam sections were reduced to 105 × 105 mm. The loading protocol used for the reversed cyclic tests was based on the international standard

ISO 21581.[9] The lateral load was measured by a load cell (capacity: ±50 kN, Tokyo Sokki Kenkyujo, Tokyo) and the horizontal displacements at the corner of the diaphragm were measured by electronic transducers (capacity: 100 mm, Tokyo Sokki Kenkyujo, Tokyo).

Lateral loading tests of 3D structures

Specimen structures were anchored on the steel base frame, which was tightly connected to the reinforced concrete reaction floor, and the lateral load was applied to the edge beam of the specimen by an actuator that was connected to the reinforced concrete reaction wall with a pin joint. Four sills of the specimen were anchored to the steel base frame with three M16 bolts positioned at the center and 150 mm inside from the ends, and an actuator was connected to the end of the X_1 plane with a pin joint, as shown in Fig. 1. The reason why the lateral load was applied at the edge beam instead of the center of the specimen was to observe more clearly the effects of the shear stiffness of the horizontal diaphragm on the seismic behavior of the 3D structure. Dynamic analysis, as described later, with and without eccentricity mass distribution and wall stiffness was conducted to follow up the test results.

The PSD tests were conducted by using a computer online system (Saginomiya ATC-20). Horizontal displacements were applied at the edge beam of the structure step by step by resolving the differential equation based on the displacement and the reaction force obtained at the previous step. The mass and the damping factor were assumed to be 10 tonne (t) and 2%, respectively, for all specimens. The accelerogram used for the PSD tests was the 1940 El Centro NS and the maximum acceleration was scaled up to 0.4 *g*. Horizontal displacements in the X and Y directions at the top of the specimen and the vertical displacements of each post were measured by electric transducers.

Experimental results

Horizontal diaphragm

Figure 4 shows the relationship between the lateral load and displacement of the horizontal diaphragm in cyclic tests with flexible (F) and rigid (R) diaphragms. The stiffness, yield, and ultimate loads obtained from the Japan Housing and Wood Technology Center guidelines for conventional wooden construction[10] were 3.39 kN/mm, 24.21 kN, and 39.00 kN for the rigid diaphragm (R) and 1.72 kN/mm, 11.08 kN, and 17.03 kN for the flexible diaphragm (F), respectively. The latter were 0.51, 0.46, and 0.44 times those of the former, indicating that the stiffness and the bearing capacity decrease rapidly when the nail joints in the longitudinal edge of the floor sheeting were removed.

3D structures

Figure 5 shows the time–displacement response relationships under PSD testing. Table 2 shows the maximum

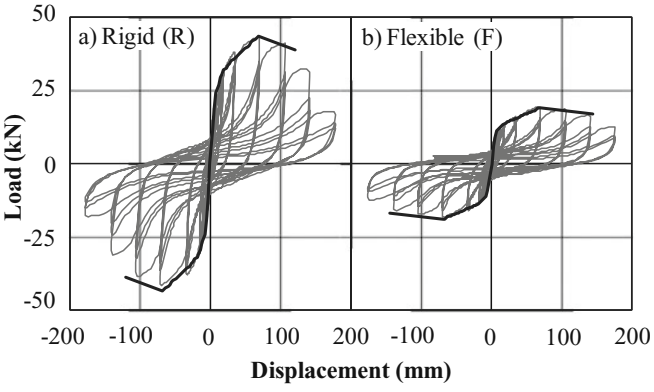

Fig. 4. Load–displacement relationship in cyclic tests for **a** the rigid diaphragm (*R*) and **b** the flexible diaphragm (*F*). The *bold line* represents the backbone curve

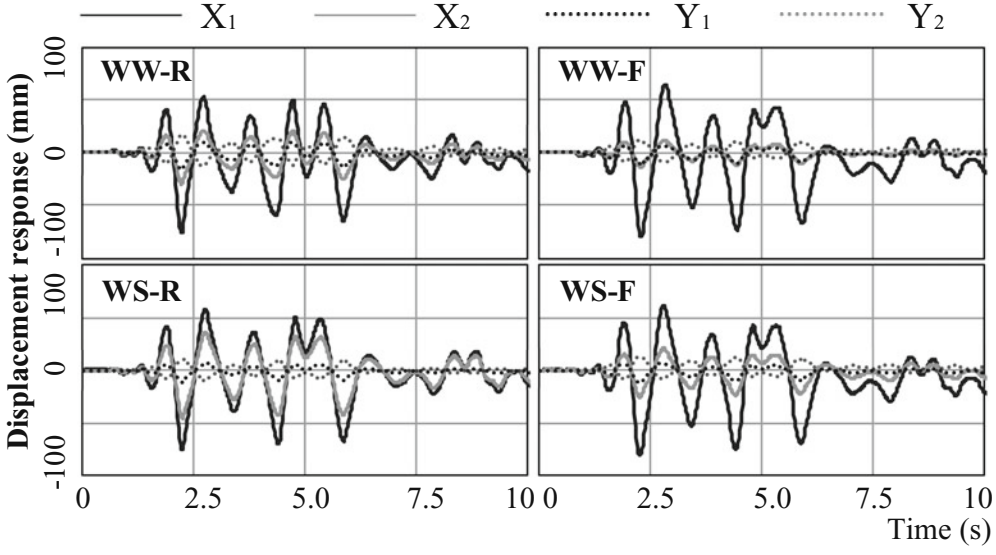

Fig. 5. Time–displacement response relationships under pseudodynamic (PSD) testing. *Black solid lines*, *gray solid lines*, *black dotted lines*, and *gray dotted lines* represent the X_1, X_2, Y_1, and Y_2 planes, respectively

Table 2. Displacement response of each plane and the horizontal diaphragm deformation angles θ_x, θ_y, and γ when the displacement of the X_1 plane was at maximum

	Time (s)	X_1 (mm)	X_2 (mm)	Y_1 (mm)	Y_2 (mm)	θ_x (rad)	θ_y (rad)	θ_x/θ_y	γ (rad)
WW-R	2.72	52.4	21.1	10.2	–12.7	1/96	1/131	0.73	1/358
	2.22	–76.1	–29.7	–16.7	16.6	1/65	1/90	0.72	1/229
WW-F	2.82	64.4	11.5	6.8	–9.2	1/57	1/188	0.30	1/81
	2.28	–80.0	–13.7	–11.5	11.9	1/45	1/128	0.35	1/70
WS-R	2.76	58.3	35.5	6.7	–10.1	1/132	1/179	0.73	1/494
	2.24	–75.4	–45.2	–11.3	10.7	1/99	1/136	0.73	1/365
WS-F	2.78	61.3	20.5	6.4	–8.8	1/74	1/198	0.37	1/117
	2.26	–81.3	–25.6	–11.7	12.7	1/54	1/123	0.44	1/96

See Fig. 6 for the definitions of θ_x ,θ_y, and γ

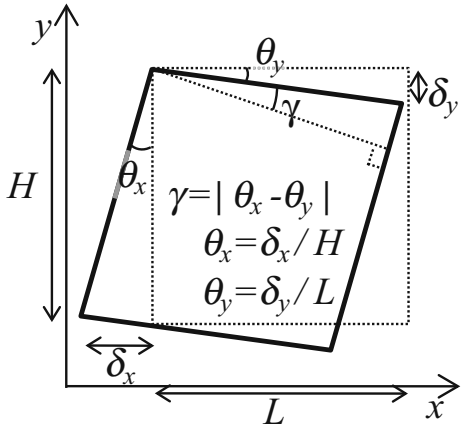

Fig. 6. Definition of θ_x, θ_y, and shear deformation angle γ

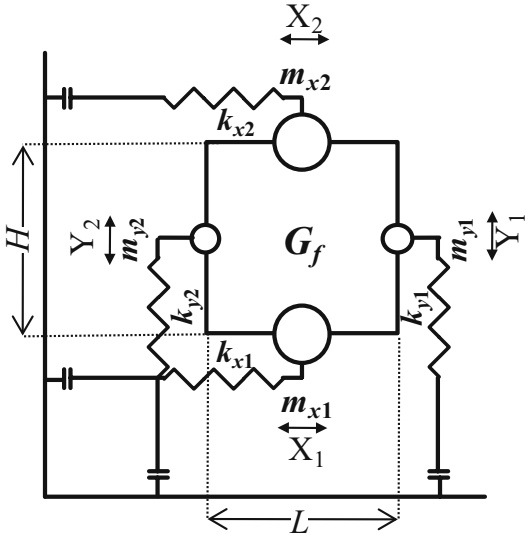

Fig. 7. Plan view of the lumped-mass model for a three-dimensional specimen

displacement responses in the X_1 plane in the positive and negative directions and those of other planes when the displacement in the X_1 plane was maximum; the definitions of θ_x, θ_y, and the shear deformation angle γ are shown in Fig. 6. Specimens with rigid diaphragms (WW-R, WS-R) and flexible diaphragms (WW-F, WS-F) showed almost the same maximum displacement response at the X_1 plane. However, the average maximum displacement response in the positive and negative directions at the X_2 plane of specimens WW-R and WS-R were 40% and 60% of those at the X_1 plane, respectively, and the maximum displacement response at the X_2 plane of specimens WW-F and WS-F were 17% and 32% of those at the X_1 plane, respectively. The shear deformation angles of the horizontal diaphragm for WW-R and WS-R were 1/229 rad and 1/365 rad, and those of specimens WW-F and WS-F were 1/70 rad and 1/96 rad, respectively. The ratios of θ_x to θ_y of the horizontal diaphragm of specimens WW-R and WS-R were 0.72 and 0.73 on an average for positive and negative displacements, and those of specimens WW-F and WS-F were 0.33 and 0.40, respectively.

This indicates that the shear force transmission from the X_1 plane to the X_2 plane decreased considerably when the nail joints in the longitudinal edge of floor sheathing were removed. Therefore, the principle deformation of the rigid diaphragm (R) is torsion, while the principle deformation of the flexible diaphragm (F) is shear deformation.

Dynamic analysis

Modeling of 3D structures

A lumped-mass model with nonlinear springs, as shown in Fig. 7, was assumed for the dynamic analysis. The model consisted of four masses (m_{x1}, m_{x2}, m_{y1}, and m_{y2}) supported by four nonlinear springs (k_{x1}, k_{x2}, k_{y1}, and k_{y2}) that represent the four vertical walls. These masses are connected to each other with a stiffness matrix representing the horizontal diaphragm. It was assumed that the horizontal diaphragm deforms as a parallelogram and has linear shear stiffness of G_f. The stiffness matrix for the horizontal diaphragm K_f is expressed as follows:

$$K_f = G_f \times \begin{bmatrix} \frac{L}{H} & -\frac{L}{H} & 1 & -1 \\ -\frac{L}{H} & \frac{L}{H} & -1 & 1 \\ 1 & -1 & \frac{H}{L} & -\frac{H}{L} \\ -1 & 1 & -\frac{H}{L} & \frac{H}{L} \end{bmatrix}$$

where G_f is the shear stiffness of the diaphragm and L and H are the length and depth of the diaphragm, respectively.[11–14] Shear walls composing the structure were modeled with the hysteresis model proposed in previous studies,[4,5,15] including Foschi's model[16] for the backbone curves and the slip model for unloading and reloading, as shown in Fig. 8. The model is defined by the following expressions:

$$P = (P_0 + C_2 x)(1 - e^{-C_1 \times x / P_0}) \quad (1)$$

$$P = P_m - C_3 |x - D_m| \quad (2)$$

$$k_1/k = C_4 \times X_m C_5 + 1 \quad (3)$$

$$k_2/k_0 = 1 - C_6 |X_m - X_0| C_7 \quad (4)$$

$$k_3/k = C_8 \times X_m C_9 + 1 \quad (5)$$

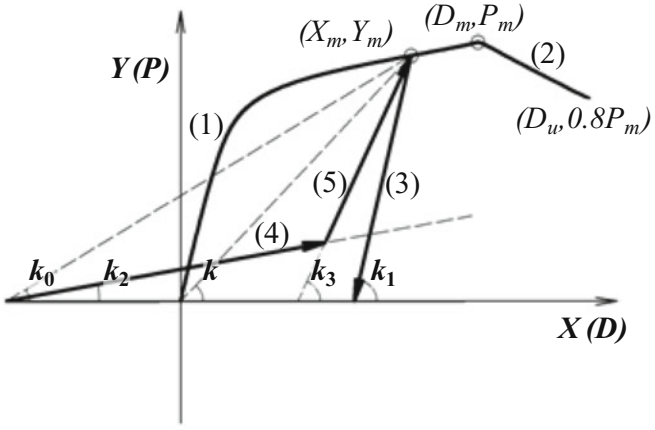

Fig. 8. Hysteresis model of shear walls. *Numbers in parentheses* correspond to the equation number in the text: (1) loading on the backbone curve up to the maximum load, (2) loading on the backbone curve above the maximum load, (3) unloading from the peak on the backbone curve, (4) reloading with a soft spring, (5) reloading toward the previous peak with a hard spring

Parameters obtained from the racking tests of shear walls with openings in the previous study were applied to the dynamic analysis of the structures. Backbone curves of the horizontal diaphragm were also modeled with Foschi's model; however the load–displacement relation was assumed to be linear, the slope of which was defined by the point on the backbone curve with the maximum displacement ever experienced. The model parameters P_0, C_1, C_2, and C_3 were obtained from the racking test of the horizontal diaphragm as shown in Table 3.

Time history earthquake response analysis

Lumped-mass time-history earthquake response analysis was conducted on the tested structures. The mass m_{x1} was set at 10 t, and the other masses m_{x2}, m_{y1}, and m_{y2} were assumed to be almost zero. The same accelerogram as used in the PSD tests, 1940 El Centro NS scaled up to 0.4 g , was applied to the dynamic analysis. The damping factor was set at 2%. Additional calculations with different eccentricities were conducted to follow up the test results.

First, the dynamic analyses were conducted on specimen WW and specimen WS with the same conditions as the former analysis by varying the masses m_{x1} and m_{x2} from 0 to 10 t, respectively, so that the sum of m_{x1} and m_{x2} was kept at 10 t. In this procedure, the eccentricity rate[10] of specimens WW and WS varied from 0 to 0.81 and from 0 to 0.73, respectively.

Second, dynamic analysis was conducted on specimen WW with masses m_{x1} and m_{x2} kept at 5 t each and the resistance factor of the walls in the X_1 and X_2 planes varied from 15% to 185% of the original wall (W) so that the sum of the stiffness and resistance of walls in the X_1 and X_2 planes was twice those of wall (W). In this procedure, the eccentricity rate varied from 0 to 0.52.

Results and discussion

Comparison of simulation with experimental results

Figure 9 shows the horizontal displacement responses of the X_1 and X_2 planes in the PSD tests and the simulation. It

Table 3. Hysteresis parameters of wall hysteresis and horizontal diaphragms for use in Eqs. 1–5

		P_0 (N)	C_1 (N/mm)	C_2 (N/mm)	C_3 (N/mm)	D_m (mm)	
Wall parameters	W (window)	17500	1810	99.2	76.5	100	
	S (slit)	16100	1360	47.4	49.0	100	
		C_4	C_5	C_6	C_7	C_8	C_9
	Common	0.210	0.628	0.120	0.323	0.0137	1.02
		P_0 (N)	C_1 (N/mm)	C_2 (N/mm)	C_3 (N/mm)	D_m (mm)	
Horizontal diaphragm parameters	R (rigid)	28410	5421	221	–	68.76	
	F (flexible)	11790	2965	104	–	69.90	

The wall parameters are quoted from Yasumura and Yasui[5]
The values of C_4–C_9 were the same for both types of wall

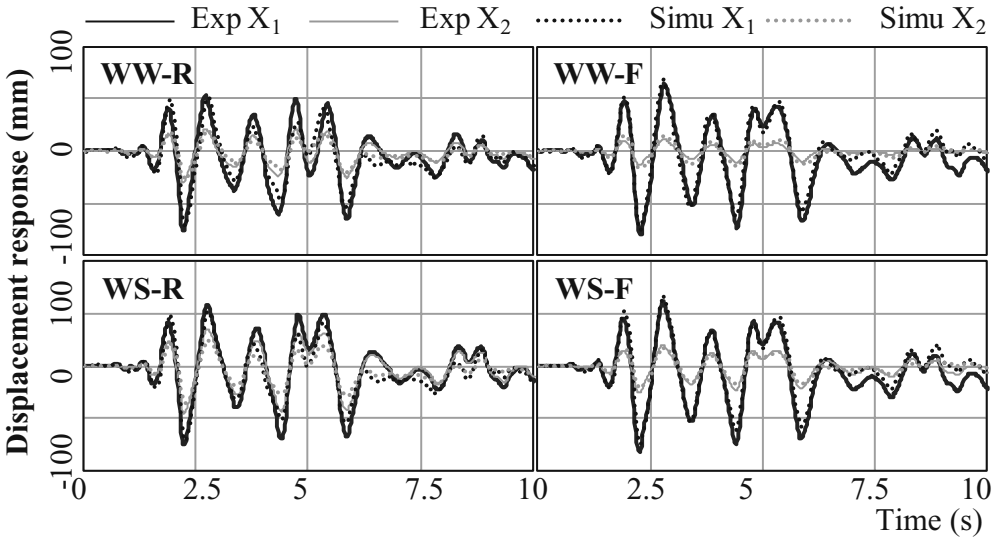

Fig. 9. Displacement responses at the X_1 and X_2 planes in the PSD tests and simulation results. *Black solid lines* and *gray solid lines* are the experimental results for the X_1 and X_2 planes, respectively. *Black dotted lines* and *gray dotted lines* are the simulation results for the X_1 and X_2 planes, respectively

Table 4. Displacement response of each plane and the horizontal diaphragm deformation angle γ when the displacement of the X_1 plane was at maximum for structure WW-R

		Time (s)	X_1 (mm)	X_2 (mm)	Y_1 (mm)	Y_2 (mm)	γ (rad)
Positive	Experiment	2.72	52.4	21.1	10.2	–12.7	1/358
	Simulation	2.76	51.6	19.2	11.9	–11.9	1/347
	Ratio		1.02	1.10	0.86	1.07	0.97
Negative	Experiment	2.22	–76.1	–29.7	–16.7	16.6	1/229
	Simulation	2.26	–71.3	–26.5	–17.4	17.4	1/304
	Ratio		1.07	1.12	0.96	0.95	1.33

Table 5. Displacement response of each plane and the horizontal diaphragm deformation angle γ when the displacement of the X_1 plane was at maximum for structure WW-F

		Time (s)	X_1 (mm)	X_2 (mm)	Y_1 (mm)	Y_2 (mm)	γ (rad)
Positive	Experiment	2.82	64.4	11.5	6.8	–9.2	1/81
	Simulation	2.80	68.7	14.3	8.5	–8.5	1/80
	Ratio		0.94	0.80	0.80	1.08	0.99
Negative	Experiment	2.28	–80.0	–13.7	–11.5	11.9	1/70
	Simulation	2.28	–75.5	–16.1	–9.7	9.7	1/75
	Ratio		1.06	0.85	1.19	1.23	1.07

Table 6. Displacement response of each plane and the horizontal diaphragm deformation angle γ when the displacement of the X_1 plane was at maximum for structure WS-R

		Time (s)	X_1 (mm)	X_2 (mm)	Y_1 (mm)	Y_2 (mm)	γ (rad)
Positive	Experiment	2.76	58.3	35.5	6.7	–10.1	1/494
	Simulation	2.78	52.6	23.8	10.3	–10.3	1/370
	Ratio		1.11	1.49	0.65	0.98	0.75
Negative	Experiment	2.24	–75.4	–45.2	–11.3	10.7	1/365
	Simulation	2.26	–70.9	–35.6	–13.2	13.2	1/334
	Ratio		1.06	1.27	0.86	0.81	0.91

Table 7. Displacement response of each plane and the horizontal diaphragm deformation angle γ when the displacement of the X_1 plane was at maximum for structure WS-F

		Time (s)	X_1 (mm)	X_2 (mm)	Y_1 (mm)	Y_2 (mm)	γ (rad)
Positive	Experiment	2.78	61.3	20.5	6.4	–8.8	1/117
	Simulation	2.80	67.5	17.5	8.3	–8.3	1/90
	Ratio		0.91	1.17	0.77	1.06	0.77
Negative	Experiment	2.26	–81.3	–25.6	–11.7	12.7	1/96
	Simulation	2.28	–74.7	–20.5	–9.3	9.3	1/84
	Ratio		1.09	1.25	1.26	1.36	0.88

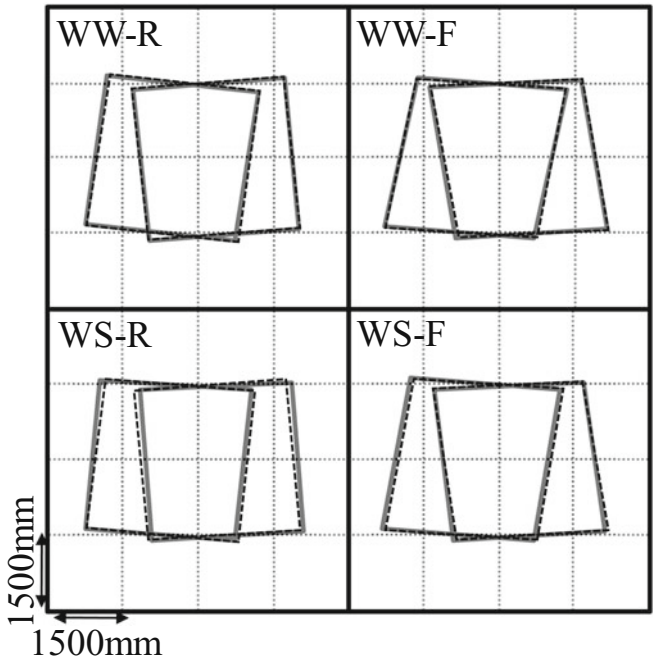

Fig. 10. Deformation of the horizontal diaphragm in the PSD tests and the simulation results. The deformation in the X and Y directions are magnified by ten. *Gray lines* indicate experimental results and *black lines* indicate the simulation results

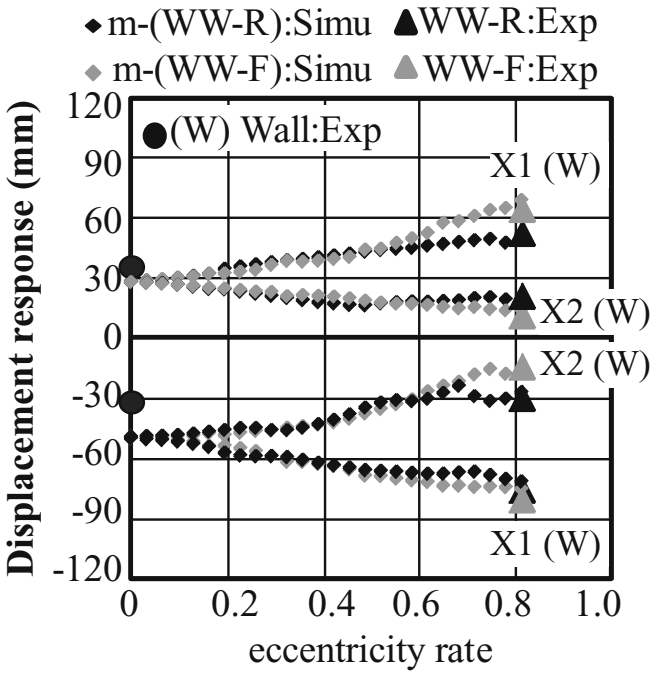

Fig. 11. Maximum displacement response–eccentricity rate relationship, where *m-(WW-R)* and *m-(WW-F)* are the displacement responses in the simulation in which the mass ratio between the X_1 and X_2 planes varied. *Triangles* indicate PSD test results of specimens WW-R and WW-F, *circles* indicate the PSD test results of wall W from Yasumura and Yasui[5]

indicates that the simulation agreed comparatively well with the PSD test results. Tables 4–7 shows that the displacement responses of the X_1, X_2, Y_1, and Y_2 planes at the time of peak displacement response agreed comparatively well with the PSD test results, except for WS-R.

In specimen WS-R, the ratios of positive (tensile) peak displacement responses in the PSD test to simulations in the X_2 and Y_1 planes were 1.49 and 0.65, respectively. The distinction between the experimental results and simulation results was as large as 35%–49%. It is supposed that the torsional displacement might be restrained by the tensile force applied at the end of the edge beam.

Figure 10 shows the deformation of the horizontal diaphragm in the PSD tests and the simulation at the time of the peak displacement in the X_1 plane, as shown in Tables 4–7. The horizontal displacements in the X and Y directions are magnified by a factor of ten. It is noted that the simulation predicts quite well the deformation of the horizontal diaphragm in the PSD tests.

Influence of the eccentricity on the earthquake response

Figures 11 and 12 show the relation between the maximum displacement response and the eccentricity rate with the sum of the masses in the X_1 and X_2 planes kept at 10 t, and the ratio of the mass in the X_2 plane to that in the X_1 plane varied from 0 to 1. The eccentricity rate of specimens WW and WS varied from 0 to 0.81 and from 0 to 0.73, respectively. The PSD tests described in the "Lateral loading test of 3D structures" section represent the extreme case in which the lateral load was applied at the end beam, giving eccentricity rates of 0.81 for WW specimens and 0.73 for WS specimens. The ratio of the maximum displacement response

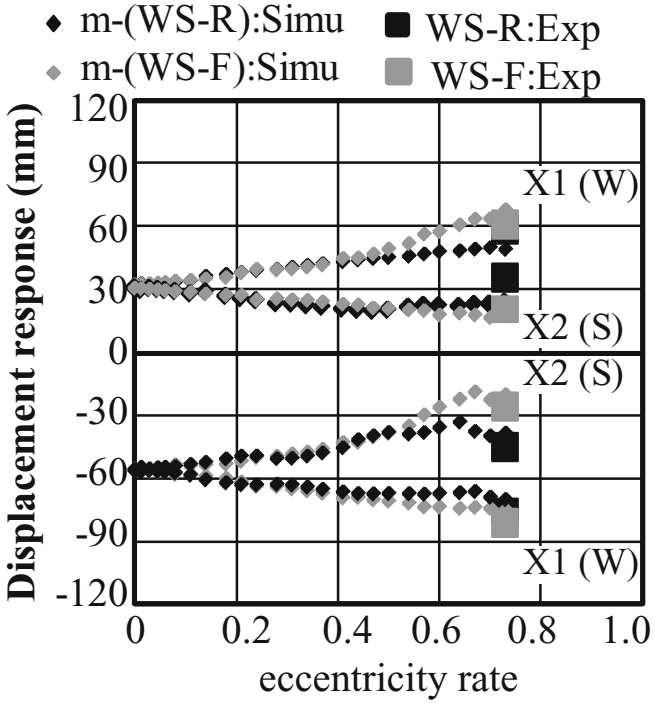

Fig. 12. Maximum displacement response–eccentricity rate relationship, where m-(WS-R) and m-(WS-F) are the same as indicated in Fig. 11. *Squares* represent the PSD test results of specimens WS-R and WS-F

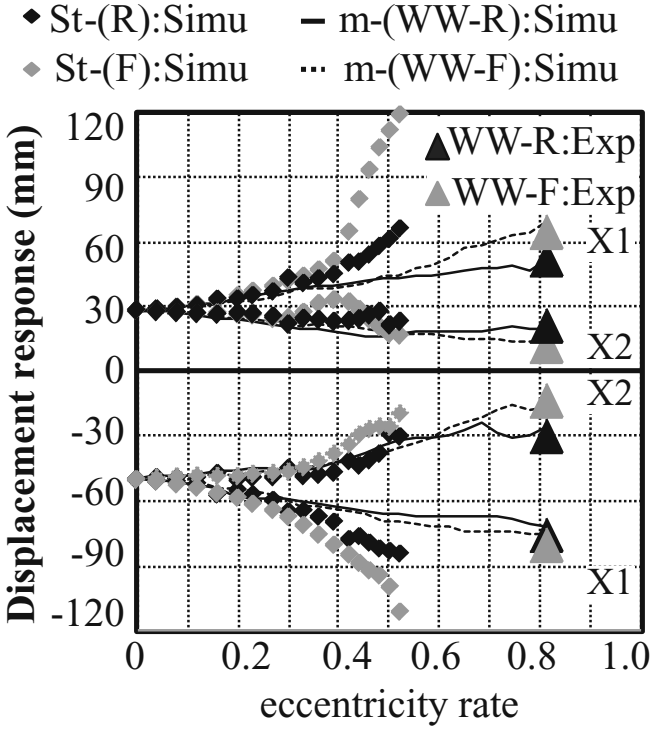

Fig. 13. Maximum displacement response–eccentricity rate relationship, where *St-(R)* and *St-(F)* stand for displacement responses in the simulation in which the wall resistance between the X_1 and X_2 planes varied

in the X_1 plane to that of the X_2 plane was greater than 2 when the eccentricity rates of specimens WW-R, WW-S, WS-R, and WS-S were 0.36, 0.45, 0.41, and 0.47, respectively. The ratio of maximum displacement response in specimen WW with a flexible diaphragm (F) to that of the specimen with a rigid diaphragm (R) was at most 1.37, which occurred when the mass was positioned at one edge of the specimen.

Figure 13 shows the relationship between the eccentricity rate and maximum displacement response, together with the results as shown in Fig. 11, when the wall resistant ratio at the X_2 plane to that of the X_1 plane varied from 1.0 to 12.33. The maximum displacement response by changing the wall resistant ratio showed almost the same tendency as that obtained by changing the mass ratio up to an eccentricity rate of 0.3; however, the maximum displacement response increased markedly beyond an eccentricity rate of 0.4.

Conclusions

The results obtained in this study can be summarized as follows. Pseudodynamic (PSD) tests showed that the shear force transmission from the X_1 plane to the X_2 plane decreased considerably when the nails in the longitudinal edge of the floor sheathing were removed. Therefore, the principle deformation of the rigid diaphragm (R) was torsion, while that of the flexible diaphragm (F) was shear deformation. The simulated values of the displacement responses of the X_1, X_2, Y_1, and Y_2 planes at the time of peak displacement response of the X_1 plane agreed well with the PSD test results. The ratio of the maximum displacement responses in the X_1 plane to that of the X_2 plane was greater than 2 when the eccentricity rate of specimens WW-R, WW-S, WS-R, and WS-S were 0.36, 0.45, 0.41, and 0.47, respectively. The ratio of maximum displacement response in a WW structure with a flexible diaphragm (F) to that with a rigid diaphragm (R) was at most 1.37 and occurred when the mass was located at one edge of the specimen. The maximum displacement response on changing the wall resistant ratio showed almost the same tendency as that obtained by changing the mass ratio up to an eccentricity rate of 0.3; however, the maximum displacement response increased markedly beyond an eccentricity rate of 0.4. The simulation predicted quite well the earthquake responses of the structures. The lumped-mass 3D model proposed in this study is suitable for conducting a parameter study on the 3D dynamic behavior of timber structures.

Acknowledgments The authors appreciate financial support of the Grants-in-Aid for Scientific Research "Category C" Monbu Kagakusho and JSPS.

References

1. Shing PB, Nakashima M, Bursi OS (1996) Application of pseudodynamic test method to structural research. Earthq Spectra 12:29–56
2. Kamiya F, Sugimoto K, Mii N (1996) Pseudo dynamic test of sheathed wood walls. In: Proceedings of the 1996 IWEC, vol 2. Omnipress, Madison, pp 187–194

3. Kawai N (1998) Pseudo-dynamic test on shear walls. In: Proceedings of the 5th WCTE, vol 1, August, 1998, EPF Lausanne, Montreux, Switzerland, pp 412–419
4. Yasumura M (2001) Evaluation of damping capacity of timber structures for seismic design. In: Proceedings of the 34th CIB-W18, Venice, Italy, paper 34-15-3, pp 1–9
5. Yasumura M, Yasui S (2006) Pseudodynamic tests and earthquake response analysis of timber structures I: plywood-sheathed conventional wooden walls with opening. J Wood Sci 52:63–68
6. Yasumura M, Kamada T, Iimura Y, Uesugi M, Daudeville L (2006) Pseudodynamic tests and earthquake response analysis of timber structures II: two-level conventional wooden structures with plywood sheathed shear walls. J Wood Sci 52:69–74
7. Japan Housing and Wood Technology Center (2003) The testing method of metal fastenings and fasteners for wooden construction (in Japanese). Japan Housing and Wood Technology Center, Tokyo
8. Japan Agricultural Standard (2008) JAS for plywood (in Japanese). JAS, Tokyo
9. ISO (2010) ISO 21581–2010: timber structures – static and cyclic lateral load test method for shear walls. ISO, Geneva
10. Japan Housing and Wood Technology Center (2001) Allowable strength design for Japanese conventional construction (in Japanese). Japan Housing and Wood Technology Center, Tokyo
11. Richard N, Yasumura M, Davenne L (2003) Prediction of seismic behavior of wood-framed shear walls with openings by pseudodynamic test and FE model. J Wood Sci 49:145–151
12. Yasumura M, Uesugi M, Luc D (2006) Estimating 3D behaviour of conventional timber structures with shear walls by pseudo-dynamic test. In: Proceedings of the 37th CIB-W18, August 30–Septmeber 3, Edinburgh, Scotland
13. Richard N, Yasumura M (2008) Dynamic model for 3D timber structures with plywood sheathed shear walls. In: Proceedings of the 10th WCTE, June 2–5, Miyazaki, Japan
14. Yasumura M, Nicolas R, Luc D, Uesugi M (2006) Estimating seismic performance of timber structures with plywood-sheathed walls by pseudo-dynamic tests and time-history earthquake response analysis. In: Proceedings of the 9th WCTE, August 6–10, Portland, OR, USA
15. Yasumura M (2003) Pseudo-dynamic tests on conventional timber structures with shear walls. In: Proceedings of the 36th CIB-W18, August 11–14, Colorado, USA
16. Foschi RO (1974) Load–slip characteristics of nails. Wood Sci 7(1):69–76